Effects of target polarization in electron elastic scattering off endohedral $A@C_{60}$

V. K. Dolmatov,[1] M. Ya. Amusia,[2,3] and L. V. Chernysheva[3]
[1]*University of North Alabama, Florence, Alabama 35632, USA*
[2]*Racah Institute of Physics, Hebrew University, 91904 Jerusalem, Israel*
[3]*A. F. Ioffe Physical-Technical Institute, 194021 St. Petersburg, Russia*
(Received 22 September 2016; published 30 January 2017)

We have developed an efficient approximation to describe the low-energy electron elastic scattering off an endohedral fullerene $A@C_N$. It accounts for polarization of $A@C_N$ by incoming electrons without reference to complicated details of the electronic structure of C_N itself. The developed approach has permitted us to unravel spectacular $A@C_N$ polarization effects in low-energy $e^- + A@C_N$ elastic scattering, particularly the effects due to interelectron interaction between the electrons of both C_N and A. We show that contribution of a single atom A remains unscreened by the multiatomic C_N despite the fact that the projectile's wavelength is bigger than the size of the target. Inclusion of A and C_N polarizability interference leads to violation of the previously predicted phase additivity rule. The partial scattering cross sections acquire prominent Ramsauer-type minima which, however, disappear in the total cross section. The study reveals notable trends in $e^- + A@C_N$ elastic scattering versus the polarizability of an encapsulated atom. We also predict the existence of certain negative ions $A@C_N{}^-$. We chose Ne, Xe, and Ba as atoms A, and C_{60} as the endohedral C_N, as the case study. The work focuses on a reasonable compromise between the qualitative and quantitative aspects of the problem in general rather than on carrying out detailed calculations for one particular system.

DOI: 10.1103/PhysRevA.95.012709

I. INTRODUCTION

Electron elastic scattering off different quantum targets is an important fundamental process that is of great significance to the basic and applied sciences and technologies. Among targets of essential current interest are endohedral fullerenes $A@C_N$ that consist of an atom A located inside the hollow interior of a molecule C_N constructed from $N \gg 1$ carbon atoms. To date, however, the knowledge on electron elastic scattering by such quantum targets as $A@C_N$ is rudimentary. This is not accidental, since the comprehensive description of electron scattering, especially in the low-energy region, by a multielectron target is too challenging for theorists even with regard to a free atom, not to mention such a complicated and multifaceted object as $A@C_N$. This is the reason why so far there have been only a few attempts undertaken by theorists [1–5] to advance into the world of low-energy electron scattering off $A@C_N$.

At first glance, the addition of a single relatively small atom inside a fullerene should not affect essentially electron elastic scattering off the latter, since the presence of an additional atom inside C_N alters only negligibly the total size of the system under consideration. In contrast, the earlier performed quantum-mechanical study [1] of this process, carried out in the framework of a model static Hartree-Fock (HF) approximation, demonstrated that the above assumption is incorrect. It appears that addition of an atom inside the hollow space of a fullerene, exemplified by C_{60} ($N = 60$), leads to remarkable alterations of electron scattering. Note that C_{60} is spherical, which makes it an ideal candidate for studies, for which reason it is the most often discussed and investigated fullerene from the fullerenes' C_N family.

Quantum-mechanical exchange between the incoming and target's electrons, as well as target's polarization caused by a projectile electron is of importance to low-energy electron elastic scattering off $A@C_N$, just as it is to electron-atom collisions. References [1–3] considered exchange in the framework of a model static Hartree-Fock (HF) approximation. In addition, Ref. [3] demonstrated the prominent role of the fullerenes' polarizability upon low-energy electron scattering by $A@C_N$. Results of Refs. [1–3] demonstrated that, due to quantum interference, the impact of the atom A on electron scattering off $A@C_N$ is, counterintuitively, not screened at all, presenting structures in corresponding differential and total electron elastic-scattering cross sections. Furthermore, Refs. [2,3] formulated the rule of scattering-phase additivity, where a role of the atom A in a $e^- + A@C_{60}$ scattering process turns out to be essential. The rule states that the scattering phase of a partial electronic wave ℓ scattered off endohedral $A@C_N$ equals, to a good approximation, the sum total of the scattering phases of electrons scattered by the atom A and the C_N fullerene itself. This rule has to be valid for any weakly bound multiatomic target as well. Moreover, results of Refs. [1–3] demonstrated that there exist certain regions of electron energy where scattering off free A even dominates over scattering by $A@C_{60}$.

The polarizability of a highly deformable object such as a fullerene has to affect the $e^- + A@C_{60}$ process. Reference [3] suggested a method that permits to account for the C_N polarizability in the scattering process by expressing the C_N polarization potential via its polarizability. This polarization potential is in addition to the static potentials of A and C_N in the Schrödinger equation for the incoming electron. The impact of the C_{60} polarization on $e^- + A@C_{60}$ scattering proved to be very important.

Reference [4] unveiled a prominent influence of the polarizability of the encapsulated atom A itself on the entire $e^- + A@C_{60}$ scattering process. Unexpectedly, despite the smallness of A and its polarizability compared to those of C_{60}, we found that the effect was far from being negligible. To demonstrate both the existence and strength of the impact

of the polarizability of the encapsulated atom A itself on $e^- + A@C_{60}$ elastic scattering, we regarded, in Ref. [4], the fullerene C_{60} as a nonpolarizable target, but unfroze the encapsulated atom A, i.e., treated as a polarizable object. Then, to account for the atomic polarizability, we utilized the Dyson formalism [6,7] for the self-energy part of the Green's function of a scattered electron to calculate the scattering phases and partial and total cross section of the $e^- + A@C_{60}$ reaction. Results of Refs. [3,4] demonstrated that the account of polarizabilities of A and C_{60} independently preserves the scattering phase additivity rule. On the other hand, those studies demonstrated the necessity to take into account both polarizabilities simultaneously. To meet the goal, i.e., to account for polarization of both the atom A and C_{60}, as well as to couple electron excitations of the atom A with electron excitations of C_{60}, the reference to complicated details of the electronic structure of C_{60} itself was thought to be absolutely needed. It remained unclear how to overcome this drawback in an efficient and yet physically transparent way.

The work [5] was a step to overcome the drawback of Refs. [1–4]. It suggested a rather simple way to take into account polarizabilities of both the atom A and C_{60} simultaneously in the calculation of $e^- + A@C_{60}$ scattering. Reference [5] provided a hint on a possible role of interference of polarizabilities by demonstrating that its account can lead to strong effects in low-energy $e^- + A@C_{60}$ scattering, including the violation of the scattering phase additivity rule.

The present paper elaborates, on the basis of results of Refs. [3–5], the approach that accounts for the mutual impact of the polarizabilities of the atom A and C_{60} on $e^- + A@C_{60}$ scattering both independently and via the interference of the polarizabilities. By choosing Ne, Xe, and Ba as the encapsulated atoms, we study how the increase in the polarizability of the atom A affects the entire process of $e^- + A@C_N$ scattering. We extrapolate the calculated scattering phases to the zero electron energy in order to disclose the bound states that result in the emergence of certain fullerene anions $A@C_N^-$. Entirely, we build, in the present work, a theory that accounts for the important effects, especially, we stress, for polarization effects due to coupling between the electrons of C_{60} and A on $e^- + A@C_N$ scattering without the need to know complicated details of the electronic structure of C_{60} itself. The theory employs certain reasonable simplifications that may affect quantitative aspects of results. However, the primary focus of the work is more on a qualitative aspect of the problem in general rather than on the performance of detailed calculations for one particular system. This is why the present study is performed on the basis of a reasonable compromise between qualitative and quantitative aspects of the problem. Namely, we account as rigor as we can for the effects which we can address and know they cannot be ignored, but employ a less quantitative approach to account for other effects, albeit important as well, for which a detailed theory is yet unavailable. Anyway, in the absence of experimental data on low-energy $e^- + A@C_{60}$ elastic scattering, which is a present situation in the field, it would remain unverified how detailed a detailed calculation would be, so focusing on that is, most likely, premature at present.

We use atomic units (a.u.) throughout the text, assuming the electronic charge e^-, mass m, and Planck's constant $\hbar$ are equal to unity: $|e^-| = m = \hbar = 1$.

II. THEORETICAL CONCEPTS

To give the reader a preview of how the problem of $e^- + A@C_{60}$ scattering is going to be addressed in the present work, before indulging in details, the key points to mention are as follows. As the first step, the C_{60} cage is approximated by an attractive square-well (in the radial coordinate r) static potential $U_c(r)$ of certain depth U_0, inner radius r_0, and thickness Δ. As a second step, in order to account for the effect of polarization of C_{60} by an incident electron, the C_{60} cage is modeled by a modified potential $V_{C_{60}}(r) = U_c(r) + V_s(r)$. Here, $V_s(r)$ is the long-range static polarization potential of C_{60}: $V_s(r) = -\alpha/[2(r^2 + b^2)^2]$, where α is the static polarizability of C_{60} and b is a parameter of the order of r_0. Next, the wave functions of incident electrons and electrons of the encapsulated atom A are calculated in the potential $V_{A@C_{60}}(r)$ which is the sum of $V_{C_{60}}(r)$ and the atomic Hartree-Fock potential $V_A^{HF}(r)$: $V_{A@C_{60}}(r) = V_{C_{60}}(r) + V_A^{HF}(r)$. This is, of course, a simplification, because at the low collision energies considered in this paper a full multielectron and nonlocal treatment of $e^- + C_{60}$ correlation and polarization effects is needed to obtain better quantitative results. However, it is known from numerous research results on electron-atom scattering that accounting at least for the static dipole polarizability of a highly polarizable atom by incident electrons is very important and it significantly improves (although not fully) the agreement between theory and experiment. It is, therefore, reasonable to account for the impact of polarization of C_{60} on electron scattering only in the framework of a C_{60}-static dipole polarizability as well, as the first step in exploring the rich variety of polarization effects, even though the quantitative aspect of the problem itself might be affected. The thus-found functions are substituted into Dyson's equation for self-energy part of the one-electron Green's function Σ of an incident electron. In the present work, Σ is defined such that it accounts for excitations of both atomic electrons and electrons of the C_{60} cage in the presence of polarized C_{60}. Then, the Dyson equation for Σ is solved with a reasonable assumption that $r_p \gg r_0 \gg r_A$. Here, r_p is the electron-projectile distance from the enter of C_{60} and r_A is the radius of the encapsulated atom A. With the thus determined Σ, electron elastic-scattering phase shifts upon electron collision with a fully polarizable $A@C_{60}$ are found and, eventually, the electron scattering cross sections are calculated, as the last step of the study.

A. Model static HF approximation: Frozen $A@C_{60}$

In the present work, as in Refs. [1–5], the C_{60} cage is modeled by an attractive spherical potential $U_c(r)$:

$$U_c(r) = \begin{cases} -U_0, & \text{if } r_0 \leqslant r \leqslant r_0 + \Delta \\ 0 & \text{otherwise.} \end{cases} \quad (1)$$

Here, r_0, Δ, and U_0 are the inner radius, thickness, and depth of the potential well, respectively.

The wave functions $\psi_{n\ell m_\ell m_s}(\boldsymbol{r},\sigma) = r^{-1} P_{nl}(r) Y_{lm_\ell}(\theta,\phi)$ $\chi_{m_s}(\sigma)$ and binding energies ϵ_{nl} of atomic electrons are the

solutions of a system of the endohedral HF equations:

$$\left[-\frac{\Delta}{2}-\frac{Z}{r}+U_{\rm c}(r)\right]\psi_i(\boldsymbol{x})+\sum_{j=1}^{Z}\int\frac{\psi_j^*(\boldsymbol{x}')}{|\boldsymbol{x}-\boldsymbol{x}'|}\times[\psi_j(\boldsymbol{x}')\psi_i(\boldsymbol{x})-\psi_i(\boldsymbol{x}')\psi_j(\boldsymbol{x})]d\boldsymbol{x}'=\epsilon_i\psi_i(\boldsymbol{x}). \quad (2)$$

Here, n, ℓ, m_ℓ, and m_s is the standard set of quantum numbers of an electron in a central field, σ is the electron spin variable, Z is the nuclear charge of the atom, $\boldsymbol{x}\equiv(\boldsymbol{r},\sigma)$, and the integration over $\boldsymbol{x}$ implies both the integration over $\boldsymbol{r}$ and summation over σ. Equation (2) differs from the ordinary HF equation for a free atom by the presence of the $U_{\rm c}(r)$ potential in there. This equation is first solved in order to calculate the electronic ground-state wave functions of the encapsulated atom. Once the electronic ground-state wave functions are determined, they are plugged back into Eq. (2) in place of $\psi_j(\boldsymbol{x}')$ and $\psi_j(\boldsymbol{x})$ in order to calculate the electronic wave functions of scattering states $\psi_i(\boldsymbol{x})$ and their radial parts $P_{\epsilon\ell}(r)\equiv P_{\epsilon_i\ell_i}(r)$ in Eq. (2).

Corresponding electron elastic-scattering phase shifts $\delta_\ell(k)$ are then determined by referring to $P_{k\ell}(r)$ at large r:

$$P_{k\ell}(r)\to\sqrt{\frac{2}{\pi}}\sin\left(kr-\frac{\pi\ell}{2}+\delta_\ell(k)\right). \quad (3)$$

Here, $P_{k\ell}(r)$ is normalized to $\delta(k-k')$, where k and k' are the wave numbers of the incident and scattered electrons, respectively. The total electron elastic-scattering cross section $\sigma_{\rm el}(\epsilon)$ is then found in accordance with the well-known formula for electron scattering by a central-potential field:

$$\sigma_{\rm el}(k)=\frac{4\pi}{k^2}\sum_{\ell=0}^{\infty}(2\ell+1)\sin^2\delta_\ell(k). \quad (4)$$

This approach solves the problem of $e^-+A@C_{60}$ scattering in a static approximation, i.e., without account for polarization of the $A@C_{60}$ system by incident electrons.

In the literature, some inconsistency is present in choosing the magnitudes of Δ, U_0, and r_0 of the model potential $U_{\rm c}(r)$ for C_{60}, for example, $r_0=5.8$, $\Delta=1.9$ and $U_0=0.302$ a.u. [8,9] (and references therein), or $r_0=6.01$, $\Delta=1.25$, and $U_0=0.422$ a.u. [10,11], or $r_0=5.262$, $\Delta=2.9102$, and $U_0=0.2599$ a.u. [1–5,12] (originally suggested in Ref. [12]). A better choice of the parameters with an eye on e^-+C_{60} scattering was investigated in Refs. [4,13]. The conclusion was in favor of the latter set of parameters: $r_0=5.262$, $\Delta=2.9102$, and $U_0=0.2599$ a.u. This is because the chosen set of parameters leads to a better agreement between some of the most prominent features of e^-+C_{60} elastic scattering predicted by the described model and the sophisticated *ab initio* static multiconfigurational Hartree-Fock approximation [12]. Correspondingly, in the present work, $U_{\rm c}(r)$ potential is defined by $\Delta=2.9102$, $r_0=5.262$, and $U_0=0.2599$ a.u.

B. Polarizable $A@C_{60}$

1. *Polarizable A but frozen* C_{60}

Let us first account for the impact of dynamical polarization of only an atom A, encapsulated inside *frozen* C_{60}, on $e^-+A@C_{60}$ elastic scattering. This should help us, later in the paper, to appreciate the importance of the effect of C_{60} polarization, in addition to that of A, on $e^-+A@C_{60}$ scattering, to finalize the study.

In the present work, as in Ref. [4], the impact of polarization of A on $e^-+A@C_{60}$ scattering (where the C_{60} cage is frozen) is accounted on the first-principle basis by utilizing the concept of the self-energy part of the Green's function of an incident electron [6,7]. In the simplest second-order perturbation theory in the Coulomb interelectron interaction V between the incident and atomic electrons, the *irreducible* self-energy part of the Green's function $\Sigma(\epsilon)$ of the incident electron is depicted with the help of Feynman diagrams in Fig. 1.

The diagrams of Fig. 1 illustrate how a scattered electron ϵ_ℓ polarizes a j subshell of the atom by causing $j\to m$ excitations from the subshell and couples with these excited states itself via both the Coulomb direct [Figs. 1(a) and 1(b)] and exchange [Figs. 1(c) and 1(d)] interactions. Numerical calculations of electron elastic-scattering phase shifts, in the framework of this approximation, are performed with the help of the computer code from Ref. [7] labeled as SHIFT. Correspondingly, the authors refer to this approximation as the SHIFT approximation everywhere in the present paper.

A fuller account of the effect of the encapsulated-atom polarization in $e^-+A@C_{60}$ elastic scattering is determined by the *reducible* $\tilde{\Sigma}(\epsilon)$ part of the self-energy part of the electron's Green's function [7]. The matrix element of the latter are represented diagrammatically in Fig. 2.

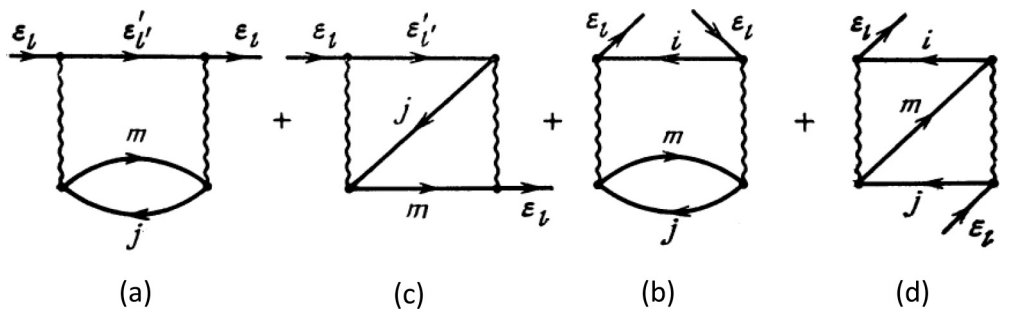

FIG. 1. The irreducible self-energy part $\Sigma(\epsilon)$ of the Green's function of a scattering electron in the second-order perturbation theory in the Coulomb interaction, referred to as the SHIFT approximation (see text). Here, a line with a right-directed arrowhead denotes either scattered states $|\epsilon_\ell\rangle$ and $|\epsilon'_{\ell'}\rangle$, or atomic excited states $|m\rangle$, a line with a left-directed arrowhead denotes the states $\langle j|$ and $\langle i|$ of a vacancy (hole) in the atom, and a wavy line denotes the Coulomb interelectron interaction V.

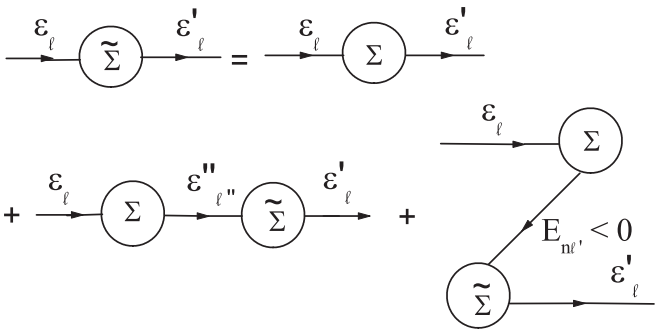

FIG. 2. The matrix element of the reducible self-energy part $\tilde{\Sigma}(\epsilon)$ of the Green's function of a scattering electron, where Σ is the irreducible self-energy part of the Green's function depicted in Fig. 1. This approximation is referred to as the SCAT approximation (see text). Note, when calculating $\langle\epsilon_\ell|\tilde{\Sigma}|\epsilon_\ell\rangle$ analytically, the summation over unoccupied discreet and integration over continuum excited states (marked as $\epsilon''_{\ell''}$) along with the summation over the occupied states in the atom marked as $E_{n\ell'}$ must be performed.

The above diagrammatic equation for $\tilde{\Sigma}$ can be written in an operator form [7], as follows:

$$\hat{\tilde{\Sigma}} = \hat{\Sigma} - \hat{\Sigma}\hat{G}^{(0)}\hat{\tilde{\Sigma}}. \tag{5}$$

Here, $\hat{\Sigma}$ is the operator of the irreducible self-energy part of the Green's function calculated in the framework of SHIFT (Fig. 1), $\hat{G}^{(0)} = (\hat{H}^{(0)} - \epsilon)^{-1}$ is the electron Green's function provided $\hat{H}^{(0)}$ is the Hamiltonian of an incident electron in a HF approximation (in the presence of the C_{60} confinement). Clearly, the equation for $\tilde{\Sigma}$ accounts for an infinite series of diagrams by coupling the diagrams of Fig. 1 in various combinations. Numerical calculation of electron elastic-scattering phase shifts in the framework of this approximation is performed with the help of the computer code from Ref. [7] labeled as SCAT. Correspondingly, this approximation is referred to as SCAT everywhere in the present paper. SCAT works well for the case of electron scattering off free atoms [7]. This gives us confidence in that SCAT is a sufficient approximation for pinpointing the impact of correlation and polarization of $A@C_{60}$ electrons on $e^- + A@C_{60}$ scattering as well.

In the framework of SHIFT or SCAT, the electron elastic-scattering phase shifts ζ_ℓ are determined as follows [7]:

$$\zeta_\ell = \delta_\ell^{\rm HF} + \Delta\delta_\ell. \tag{6}$$

Here, $\Delta\delta_\ell$ is the correlation and polarization correction term to the calculated HF phase SHIFT $\delta_\ell^{\rm HF}$ [7]:

$$\Delta\delta_\ell = \tan^{-1}(-\pi\langle\epsilon\ell|\tilde{\Sigma}|\epsilon\ell\rangle). \tag{7}$$

The mathematical expression for $\langle\epsilon\ell|\tilde{\Sigma}|\epsilon\ell\rangle$ is cumbersome. The interested reader is referred to Ref. [7] for details. The matrix element $\langle\epsilon\ell|\tilde{\Sigma}|\epsilon\ell\rangle$ becomes complex for electron energies exceeding the ionization potential of the atom scatterer, and so does the correlation term $\Delta\delta_\ell$ and, thus, the phase shift ζ_ℓ as well. Correspondingly,

$$\zeta_\ell = \delta_\ell + i\mu_\ell, \tag{8}$$

where

$$\delta_\ell = \delta_\ell^{\rm HF} + {\rm Re}\Delta\delta_\ell, \quad \mu_\ell = {\rm Im}\Delta\delta_\ell. \tag{9}$$

The total electron elastic-scattering cross section $\sigma_{\rm el}$ is then given by the expression

$$\sigma_{\rm el} = \sum_{\ell=0}^{\infty}\sigma_\ell, \tag{10}$$

where σ_ℓ is the electron elastic-scattering partial cross section [7]:

$$\sigma_\ell = \frac{2\pi}{k^2}(2\ell+1)(\cosh 2\mu_\ell - \cos 2\delta_\ell)e^{-2\mu_\ell}. \tag{11}$$

2. *Polarizable A and C_{60}: Approximation of uncoupled polarizabilities*

We now account for the effects of polarization of C_{60} by an incoming electron in addition to the encapsulated atom polarization. This is done in a simple approximate way, as is often done in atomic physics [14]. Namely, the long-range polarization potential of C_{60} is approximated by a static dipole polarization potential $V_{\rm p}(r)$:

$$V_{\rm p}(r) = -\frac{\alpha}{2(r^2+b^2)^2}. \tag{12}$$

Here, α is the static dipole polarizability of C_{60} and b is the cutoff parameter of the order of the radius of C_{60}, r_0.

In the present work, the C_{60} effective potential $V_{C_{60}}^{\rm eff}(r)$, detected by an incident electron, is approximated by the sum of the short-range potential $U_{\rm c}(r)$, Eq. (1), and the long-range polarization potential $V_{\rm p}(r)$, Eq. (12):

$$V_{C_{60}}^{\rm eff}(r) = U_{\rm c}(r) + V_{\rm p}(r). \tag{13}$$

In the given approximation, the wave functions of the ground and excited states of the atom A are calculated with the help of Eq. (2), where the potential $U_{\rm c}(r)$ is replaced by $V_{C_{60}}^{\rm eff}(r)$. Such defined wave functions are used in calculations of $e^- + A@C_{60}$ elastic-scattering phase shifts with account for dynamical polarization of the atom A in the presence of polarizable C_{60}. This is done in the framework of the above-described Dyson formalism for the self-energy part of the Green's function of an incident electrons, Eqs. (5)–(11). The determined phase shifts are plugged into Eqs. (5) and (7) to meet the goal of the study, that is to account for the impact of both *dipole static* polarization of C_{60} (in the model approximation) and *dynamical* polarization of the encapsulated atom A (on the first-principle basis) on $e^- + A@C_{60}$ scattering.

In the developed approximation, the polarizabilities of C_{60} and A are, obviously, not coupled with each other (no interelectron interaction between the electrons of A and C_{60}). This approximation is referred to as the *approximation of uncoupled polarizabilities* of C_{60} and A in the present paper.

3. *Polarizable A and C_{60}: Approximation of coupled polarizabilities*

In the present paper, the term *coupled polarizabilities* of A and C_{60} means coupling between excited configurations of A and C_{60}, both of which are caused by an incident electron. The corresponding correction to $e^- + A@C_{60}$ scattering is in addition to the above-discussed effect of uncoupled polarizabilities of A and C_{60}. In the present work, this is done, first, by

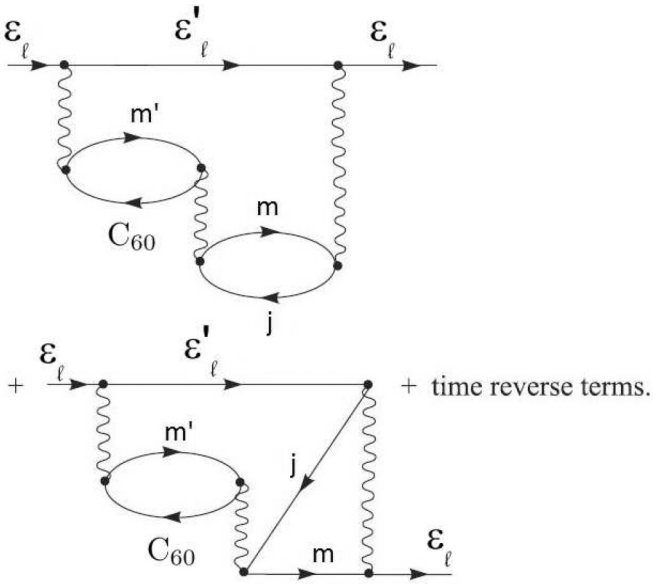

FIG. 3. The multielectron processes accounting for the interaction between excited configurations of C_{60} and A brought about by an incident electron. Lines marked as C_{60} and m' denote the core and excited states of the fullerene cage C_{60}, respectively. Other notations are the same as in Fig. 1.

adding some specific third-order terms of perturbation theory in Coulomb interaction to the *irreducible* $\Sigma(\epsilon)$ (Fig. 1). Then, thus redefined $\Sigma(\epsilon)$ is substituted into the equation for the *reducible* part of the Green's function $\tilde{\Sigma}(\epsilon)$ [Eq. (5) and/or Fig. 2]. The third-order terms in question are depicted with the help of Feynman diagrams in Fig. 3.

Strictly speaking, to calculate the terms depicted in Fig. 3, one needs to calculate wave functions of the ground and excited states of the multielectron fullerene cage C_{60}. In the present paper, we bypass this difficulty by employing a simple and yet reasonable approximation. It consist in the following. First, it takes into account that the radius r_0 of the C_{60} cage is bigger than the radius r_A of an encapsulated atom A: $r_0 > r_A$. Second, it exploits the fact that, at large distances r_p from the target (where $r_p > r_0 > r_A$), the impact of the polarization potential of C_{60} on electron scattering is accounted, to a good approximation, by the static dipole polarization potential, Eq. (12), whereas the polarization of C_{60} at smaller distances is approximately accounted by the phenomenological short-range square-well potential, Eq. (1), itself. Note, the latter being phenomenological, accounts only on the average for various virtual excitations of multiple low-energy resonances from the sea of the detached electrons of C_{60}. This potential, thus, cannot by itself predict those resonances. This leads to obvious limitation of the present theory. Hence, $r_p > r_0$, r_p being the important electron-projectile distance from the center of C_{60}. Next, as a not too strong exaggeration, let us regard that $r_p \gg r_0 \gg r_A$. Then, the Coulomb interaction between the incident electron and C_{60}'s electrons, $V(\boldsymbol{r}_p,\boldsymbol{r}_C) \propto |\boldsymbol{r}_p - \boldsymbol{r}_C|^{-1}$, and that one between the C_{60}'s electrons and electrons of the encapsulated atom A, $V(\boldsymbol{r}_A,\boldsymbol{r}_C) \propto |\boldsymbol{r}_A - \boldsymbol{r}_C|^{-1}$, turn, approximately, into the long-range dipole potentials:

$$V(\boldsymbol{r}_p,\boldsymbol{r}_C) \propto \frac{\boldsymbol{r}_p\boldsymbol{r}_C}{\boldsymbol{r}_p^3}, \quad V(\boldsymbol{r}_A,\boldsymbol{r}_C) \propto \frac{\boldsymbol{r}_A\boldsymbol{r}_C}{\boldsymbol{r}_C^3}. \tag{14}$$

Hence, the exact Coulomb interactions, represented by the first and second wavy lines in the diagrams of Fig. 3, can now be replaced by their approximate values defined by Eq. (14). This is equivalent to accounting for the impact of only dipole polarization of C_{60} on electron scattering. The impact can be expressed via the known dipole polarizability α of C_{60}, similar to how it has been done in Ref. [15]. One can show that this is equivalent to making simple replacements

$$|V|^2 \to \left|V\left[1 - \alpha(\epsilon_\ell - \epsilon'_\ell)/r_0^3\right]\right|^2 \tag{15}$$

in Figs. 1(a) and 1(c), and

$$|V|^2 \to \left|V\left[1 - \alpha(\epsilon_\ell - \epsilon'_\ell)/r_0^3\right] \times V\left[1 - \alpha(\epsilon_\ell - \epsilon_m)/r_0^3\right]\right| \tag{16}$$

in Figs. 1(c) and 1(d). Next, the recalculated $\Sigma(\epsilon)$ (Fig. 1) is substituted into Eq. (5) for $\tilde{\Sigma}(\epsilon)$. The latter concludes the problem of $e^- + A@C_{60}$ scattering in the framework of the approximation of coupled polarizabilities of C_{60} and A.

III. RESULTS AND DISCUSSION

A. Preliminary notes

First, in order the modeling of the C_{60} cage by the homogeneous spherical potential $U_c(r)$, Eq. (1), made sense, the wavelength λ of an incident electron must exceed greatly the bond length $D \approx 1.44$ Å between the carbon atoms in C_{60}. In the present work, therefore, the maximum energy of an incident electron is capped at approximately 4 eV. Up to this energy, $\lambda \gtrsim 6$ Å, so that, indeed, $\lambda \gg D$.

Second, given that the outer radius of C_{60} is approximately 8 a.u., one can easily estimate that the maximum contribution to electron scattering comes from the first five electron partial waves with ℓ ranging from 0 to 4. Correspondingly, in the present work, the maximum value of ℓ is capped at $\ell = 4$.

Third, when accounting for multipolar excitations of the electronic subshells of an encapsulated atom A by an incident electron, the performed calculations accounted for the monopole, dipole, quadrupole, and octupole excitations of outer subshells of the atoms. For the chosen in the present paper set of encapsulated atoms, these are the $6s^2$ and $5p^6$ subshells in Ba, $5p^6$ in Xe, and $2p^6$ in Ne.

Fourth, since one of the main goals of this study is to explore how both the size of an atom and its dynamical polarizability might affect electron scattering off polarizable $A@C_{60}$, the study is run along the path from the most compact to the most diffuse encapsulated atom: $e^- + Ne@C_{60} \to e^- + Xe@C_{60} \to e^- + Ba@C_{60}$.

Finally, in order to facilitate the reader to cope with various abbreviations for the utilized approximations, adopted in the present paper, these are as follows:

(1) HF stands for the model static HF approximation, where both the encapsulated atom A and the fullerene cage C_{60} are regarded as nonpolarizable targets (see Subsec. A above).

(2) SCAT(A@) marks the approximation, which accounts for polarization of only the encapsulated atom A (see Subsec. 1 of Subsec. B).

(3) SCAT(A) designates the approximation as the above one, but in relation to a free atom A.

(4) SCAT(UP) labels the approximation of uncoupled polarizabilities of C_{60} and A (see Subsec. 2 of Subsec. B).

(5) SCAT(CP) stands for the approximation of coupled polarizabilities of C_{60} and A (see Subsec. 3 of Subsec. B).

B. $e^- + \mathrm{Ne@C_{60}}$ scattering

Based on our previous HF calculated data for $e^- + A@C_{60}$ scattering [1–3], it is known that the encapsulation of Xe into the C_{60} cage practically does not change electron elastic scattering off $e^- + A@C_{60}$ compared to scattering by empty C_{60} calculated within the model static approximation. This is because the Xe atom is compact. Obviously, one can expect the same for even smaller compact atoms, like the Ne atom. In addition, the Ne atom has a smaller polarizability α than that of Xe or Ba. For example, experimental values of the static dipole polarizabilities of the ground states of Ne, Xe, and Ba are as follows: $\alpha(\mathrm{Ne}) \approx 2.67$, $\alpha(\mathrm{Xe}) \approx 27.34$, and $\alpha(\mathrm{Ba}) \approx 269$ a.u. [16]. Therefore, the study of $e^- + \mathrm{Ne@C_{60}}$ scattering makes particular sense in two respects. First, it allows us to understand better how accounting for polarization of only C_{60} affects electron elastic scattering off C_{60} doped with a compact static atom. Second, the study can shed light on whether the coupling between the *weak* polarizability of a compact atom A with the *large* polarizability of C_{60} ($\alpha \approx 850$ a.u. [15]) can have a noticeable effect on $e^- + A@C_{60}$ scattering compared to that calculated in the SCAT(UP) approximation. Common sense suggests that the effect should be negligible. However, as one of key findings of the present work, such intuitive perception turns out to be not entirely correct.

Calculated HF, SCAT(A@), SCAT(A), SCAT(UP), and SCAT(CP) data for the real parts $\delta_\ell(\epsilon)$ of phase shifts, as well as the partial $\sigma_\ell(\epsilon)$ and total $\sigma_{\mathrm{el}}(\epsilon)$ cross sections of a $e^- + \mathrm{Ne@C_{60}}$ elastic collision, are displayed in Fig. 4.

One can see that the difference between calculated model static HF data and SCAT(@A) data for all partial electronic waves is negligible. This agrees with common sense, in view of insignificant polarizability of Ne. The data also demonstrate that the polarizability of a free small-sized compact atom, like Ne, remains small upon its encapsulation inside C_{60}. Indeed, in the opposite case, the difference between calculated static HF and SCAT(A@) data would have been noticeable.

Let us now explore the calculated data for the p-, d-, f-, and g-partial electronic waves scattered off $\mathrm{Ne@C_{60}}$. One can conclude that simultaneous accounting for polarization of both Ne and C_{60} by the scattered electron [SCAT(UP) and SCAT(CP) approximations; dashed and solid lines, respectively] has a huge effect on the corresponding cross sections compared to when only polarization of Ne is accounted [SCAT(A@), dash-dotted line]. This was expected in view of a large polarizability of C_{60}. Yet, details of how the polarization of C_{60} affects $e^- + A@C_{60}$ scattering have been cleared up only in the present study, to the authors' best knowledge. Next, one can also see that the effect of coupling between the polarizabilities of Ne and C_{60} [SCAT(CP) approximation, solid line] on

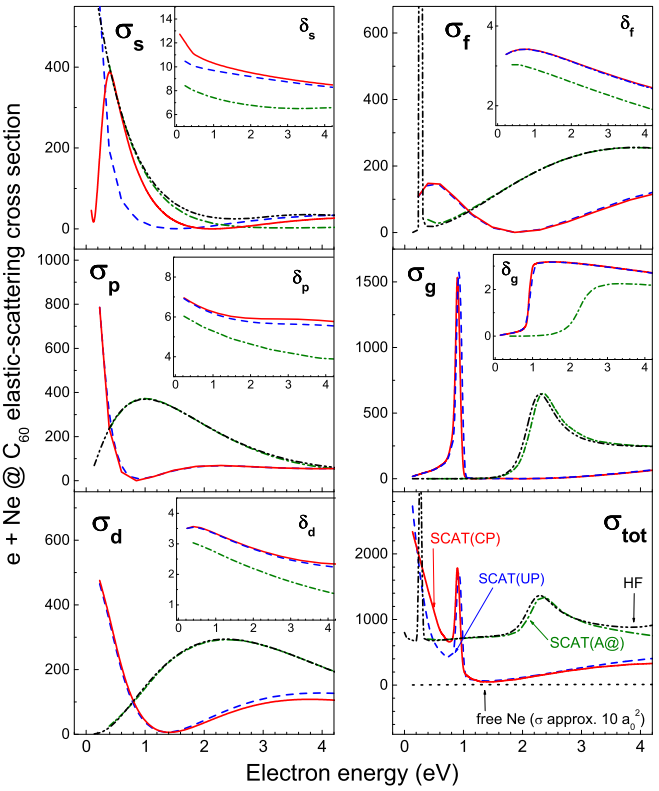

FIG. 4. Main panels: Calculated partial $\sigma_\ell(\epsilon)$ and total $\sigma_{\mathrm{el}}(\epsilon)$ cross sections (a.u.) for electron elastic scattering off $\mathrm{Ne@C_{60}}$. Insets: Real parts $\delta_\ell(\epsilon)$ of the phase shifts (in units of radians); imaginary parts $\mu_\ell = 0$ in this energy region. The used styles of the plotted lines mark results obtained in different approximation utilized in the present work, as follows: dash-dot-dot, HF; dash-dot, SCAT(A@); dots, SCAT(A) (free Ne); dash, SCAT(UP); solid, SCAT(CP) (the most complete approximation). Note, the calculated SCAT(A@) and HF data for p-, d-, and for a better part of f-partial cross sections are so close to each other that one can hardly tell one from the other.

scattering of these partial electronic waves off $e^- + \mathrm{Ne@C_{60}}$ is insignificant. Indeed, the calculated SCAT(CP) and SCAT(UP) (dashed line) data are practically identical. This, again, fits common sense, in view of a small polarizability of Ne.

However, the study finds that s scattering behaves quite differently compared to the above case of scattering of waves with higher ℓs. In contrast to the above case, we found both big quantitative and qualitative differences between calculated $\sigma_s^{\mathrm{SCAT(UP)}}$ (dashed line) and $\sigma_s^{\mathrm{SCAT(CP)}}$ (solid line). Indeed, $\sigma_s^{\mathrm{SCAT(UP)}}$ is seen to monotonically increase, whereas, in contrast, $\sigma_s^{\mathrm{SCAT(CP)}}$ develops a strong maximum with decreasing electron energy ϵ. The reason for the different behavior of $\sigma_s^{\mathrm{SCAT(CP)}}$ versus $\sigma_s^{\mathrm{SCAT(UP)}}$ becomes clear upon exploring the corresponding phase shifts. One can see that the phase shift $\delta_s^{\mathrm{SCAT(CP)}}$ (solid line on inset) crosses the value of modulo $\pi/2$ as $\epsilon \to 0$, whereas $\delta_s^{\mathrm{SCAT(UP)}}$ (dashed line on inset) does not. Correspondingly, the cross section $\sigma_s^{\mathrm{SCAT(CP)}}$ develops a resonance at low ϵ, opposite to $\sigma_s^{\mathrm{SCAT(UP)}}$, whereas the already existing Ramsauer minimum shifts towards higher energy. Note, the behavior of the phase shift $\delta_s^{\mathrm{SCAT(CP)}}$ speaks to the fact that the binding potential of $e^- + \mathrm{Ne@C_{60}}$ gets stronger when the polarizabilities of Ne and C_{60} are coupled. This results in

the emergence of an additional bound s state in the field of $e^- + \mathrm{Ne@C_{60}}$ (compared to the approximation on uncoupled polarizabilities), thereby pushing $\delta_s^{\mathrm{SCAT(CP)}}$ to a larger value than that of $\delta_s^{\mathrm{SCAT(UP)}}$, at $\epsilon \to 0$. This is in accordance with the well-known Levinson theorem: $\delta_\ell \to n_\ell \pi$ at $\epsilon \to 0$, n_ℓ being the total number of bound ℓ states in the system (valid when projectile-target electron exchange is neglected, as in the present work).

Another interesting effect relevant to s scattering is that coupling between polarizabilities of C_{60} and Ne is found to largely cancel out the strong polarization impact of C_{60} on $\sigma_s^{\mathrm{Ne@C_{60}}}$ in a broad energy region to the right of the maximum in $\sigma_s^{\mathrm{SCAT(CP)}}$ (solid line). Indeed, there, $\sigma_s^{\mathrm{SCAT(CP)}}$ differs only somewhat from both σ_s^{HF} (dash-dot-dotted line) and $\sigma_s^{\mathrm{SCAT(A@)}}$ (dash-dotted line), but it differs significantly from $\sigma_s^{\mathrm{SCAT(UP)}}$ (dashed line). We, thus, have unraveled an interesting effect. Namely, it is found that coupling of the large polarizability of C_{60} with the considerably smaller polarizability of a compact encapsulated atom can have a significant impact on scattering of at least some of electronic partial waves off $A@C_{60}$. This, in turn, affects the total electron elastic scattering cross section $\sigma_{\mathrm{tot}}^{A@C_{60}}$ as well, in the corresponding region of electron energies (cf. dash and solid lines in the right bottom panel of Fig. 4).

Next, we comment on one more interesting finding related to scattering of a g-partial electronic wave. The g wave is seen to induce a strong narrow resonance in the g-partial scattering cross section σ_g of $e^- + \mathrm{Ne@C_{60}}$ scattering. The resonance is predicted by each of the utilized approximation: HF, SCAR(@A), SCAT(UP), and SCAT(CP). The origin of this resonance in g scattering was established earlier in Refs. [4,12], where it was shown that this is a shape resonance. One can see that the resonance in the cross section σ_g, calculated both in SCAT(UP) and SCAT(CP) approximations, emerges at noticeably lower energies and becomes significantly narrower than that in σ_g calculated in the framework of HF or SCAT(@A). The emphasized difference is interesting. The fact that the g resonance emerges at the lowest energy and is the most narrow when calculated in the SCAT(CP) framework means that coupling between polarizabilities of C_{60} and A can result in a much stronger binding potential of $A@C_{60}$ than that calculated otherwise.

Lastly, the performed calculations demonstrate that accounting for polarization of $A@C_{60}$ by a scattered electron results in the emergence of near-zero minima in all partial cross sections σ_ℓs. We refer to these minima as the Ramsauer minima by analogy with the known Ramsauer minima in electron elastic-scattering cross sections of some of free atoms (e.g., Xe). The presence of Ramsauer minima in all σ_ℓs for $e^- + \mathrm{Ne@C_{60}}$ scattering might prompt one to conclude that the total scattering cross section $\sigma_{\mathrm{tot}}^{\mathrm{Ne@C_{60}}}$ could be so small that it might fall below the electron elastic-scattering cross section of free Ne, $\sigma_{\mathrm{tot}}^{\mathrm{Ne}}$, at some electron energy. This, however, does not happen, because Ramsauer minima in the partial cross sections $\sigma_\ell^{\mathrm{Ne@C_{60}}}$ for different ℓs emerge at somewhat different energies. Therefore, the minimum value of the total cross section $\sigma_{\mathrm{tot}}^{\mathrm{Ne@C_{60}}}$ remains far greater than the cross section $\sigma_{\mathrm{tot}}^{\mathrm{Ne}}$. In the present case, $\sigma_{\mathrm{tot}}^{\mathrm{Ne@C_{60}}}|_{\mathrm{min}} \approx 60$ a.u. at $\epsilon \approx 1.4$ eV, whereas the electron elastic-scattering cross section of free Ne is one order of magnitude smaller, $\sigma_{\mathrm{tot}}^{\mathrm{Ne}} \approx 6$ a.u., at 1.4 eV (cf. a solid or a dashed line with a dotted line in the right bottom panel of Fig. 4).

C. $e^- + \mathrm{Xe@C_{60}}$ scattering

We next explore changes in $e^- + A@C_{60}$ scattering with increasing size and polarizability of an encapsulated atom A which, however, is still a relatively compact atom of moderate polarizability. To meet the goal, we study $e^- + \mathrm{Xe@C_{60}}$ scattering. Corresponding calculated data are displayed in Fig. 5.

Overall important similarities in, and difference between $e^- + \mathrm{Xe@C_{60}}$ and $e^- + \mathrm{Ne@C_{60}}$ scattering surface upon comparison of Fig. 5 with Fig. 4.

We start focusing on similarities in $e^- + \mathrm{Xe@C_{60}}$ and $e^- + \mathrm{Ne@C_{60}}$ scattering. The overall impact of polarization of $\mathrm{Xe@C_{60}}$ by an incident electron on $e^- + \mathrm{Xe@C_{60}}$ scattering remains significant. It results in the corresponding partial and total cross sections that differ strongly from those calculated without regard for the polarization effect. Next, similar to s scattering off $\mathrm{Ne@C_{60}}$, the effect of coupled polarizabilities of Xe and C_{60} [SCAT(CP) approximation] impacts strongly the s scattering cross section. Indeed, this impact results

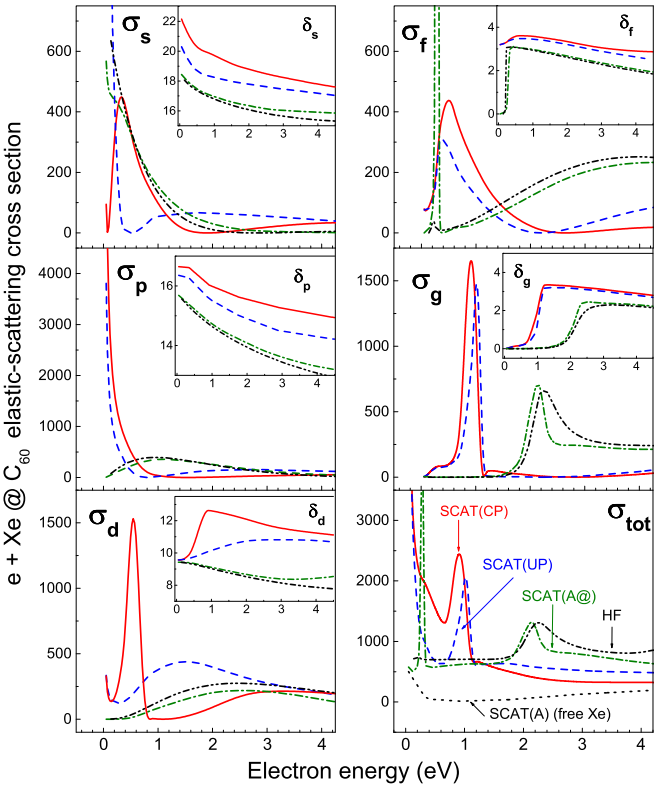

FIG. 5. Main panels: Calculated partial $\sigma_\ell(\epsilon)$ and total $\sigma_{\mathrm{el}}(\epsilon)$ cross sections (in atomic units) for electron elastic scattering off $\mathrm{Xe@C_{60}}$. Insets: Real parts $\delta_\ell(\epsilon)$ of the phase shifts (in units of radian); $\mu_\ell = 0$ in this energy region. The used styles of the plotted lines mark results obtained in different approximation utilized in the present work, as follows: dash-dot-dot, HF; dash-dot, SCAT(A@); dots, SCAT(A) (free Xe); dash, SCAT(UP); solid, SCAT(CP) (the most complete approximation).

in a strong shape resonance in $\sigma_s^{\mathrm{SCAT(CP)}}$ (solid line) below 1 eV of the electron energy. Furthermore, when coupling between polarizabilities of Xe and C_{60} is accounted in the calculation of s scattering, it largely cancels out the overall polarization impact of Xe@C_{60} on s scattering in a broad energy region to the right of the maximum in $\sigma_s^{\mathrm{SCAT(CP)}}$ (solid line). Indeed, there, the s cross section becomes about the same as the one calculated in the SCAT(A@) and HF approximations (dash-dotted and dash-dot-dotted lines). The emergence of the noted cancellation effect in two independent calculations (s scattering off Xe@C_{60} and off Ne@C_{60}) speaks to the fact that the discovered effect is not accidental. Next, coupling between polarizabilities of Xe and C_{60} results in the emergence of Ramsauer minima in corresponding σ_ℓs. Lastly, similar to $e^- + \mathrm{Ne@C_{60}}$ scattering, the total cross section $\sigma_{\mathrm{tot}}^{\mathrm{Xe@C_{60}}}$ exceeds noticeably that for electron scattering off free Xe (note, the cross section of electron elastic scattering off free Xe has its own low-energy Ramsauer minimum as well, in contrast to that for Ne).

The most striking differences between $e^- + \mathrm{Xe@C_{60}}$ and $e^- + \mathrm{Ne@C_{60}}$ scattering consist in the following. First, in contrast to a d-wave scattering off Ne@C_{60}, the d-wave scattering off Xe@C_{60} is subject to a particularly strong impact of coupled polarizabilities of Xe and C_{60}. Indeed, in the present case, the d-scattering cross section $\sigma_d^{\mathrm{SCAT(CP)}}$ (solid line) develops the intense shape resonance below of 1 eV and differs qualitatively and quantitatively from calculated data obtained in the frameworks of the SCAT(UP) (dashed line) and other utilized approximations. Second, the overall differences between calculated SCAT(UP) and SCAT(CP) electron scattering cross sections (both partial and total) are noticeably stronger in the case of $e^- + \mathrm{Xe@C_{60}}$ scattering than in $e^- + \mathrm{Ne@C_{60}}$ scattering.

In summary, the highlighted differences between $e^- + \mathrm{Xe@C_{60}}$ and $e^- + \mathrm{Ne@C_{60}}$ underpin the effect of a bigger size and greater polarizability of a compact encapsulated atom A on $e^- + A\mathrm{@C_{60}}$ scattering.

D. $e^- + \mathrm{Ba@C_{60}}$ scattering

In the earlier study of $e^- + \mathrm{Ba@C_{60}}$ scattering [4], the impact of the polarization of *only encapsulated Ba* on the scattering process was accounted in the calculations [the SCAT(A@) approximation]. This impact was found to be considerable, due to a large value of the Ba polarizability. The $e^- + \mathrm{Ba@C_{60}}$ scattering, therefore, stands out of the cases of $e^- + \mathrm{Ne@C_{60}}$ and $e^- + \mathrm{Xe@C_{60}}$ scattering. It sheds light on features of the impact of coupled polarizabilities of a highly polarizable atom and highly polarizable C_{60} on $e^- + A\mathrm{@C_{60}}$ scattering. Corresponding calculated data for $e^- + \mathrm{Ba@C_{60}}$ scattering are displayed in Fig. 6.

An interesting feature, which caught our attention in the first head, is a cancellation effect of a new quality in the scattering process, compared to electron scattering off Ne@C_{60} and off Xe@C_{60} cases. Namely, the account for the effect of coupled polarizabilities of Ba and C_{60} in the calculation has practically annihilated the overall polarization impact of Ba@C_{60} on the s-, p-, and d-partial cross sections above approximately 1.4 eV of the electron energy. This follows clearly from the comparison of calculated $\sigma_\ell^{\mathrm{SCAT(CP)}}$ (solid lines) and $\sigma_\ell^{\mathrm{HF}}$ (dash-dot-dotted lines) for $\ell = s$, p, and d. There, indeed, $\sigma_\ell^{\mathrm{SCAT(CP)}} \approx \sigma_\ell^{\mathrm{HF}}$. For a p cross section, this is true even for energies down to approximately 0.4 eV, to a good approximation. For higher ℓs, especially for the g cross section, as well as for the total cross section σ_{tot} above about 1.6 eV, calculated SCAT(CP) data are noticeably closer to HF data than to cross sections calculated by accounting for polarization of only Ba (dash-dotted line) or C_{60} (dashed line).

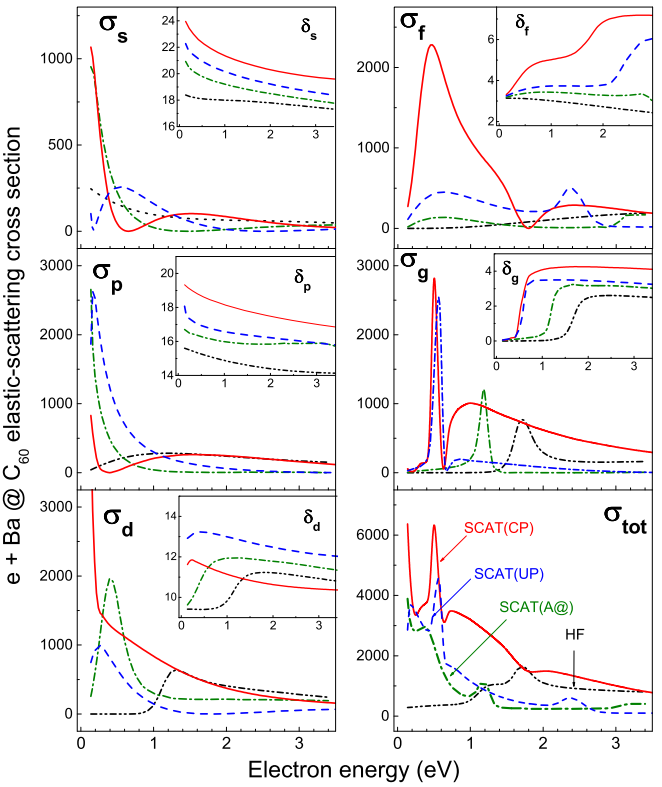

FIG. 6. Main panels: Calculated partial $\sigma_\ell(\epsilon)$ and total $\sigma_{\mathrm{el}}(\epsilon)$ cross sections (in atomic units) for electron elastic scattering off Ba@C_{60}. Insets: Real parts $\delta_\ell(\epsilon)$ of the phase shifts (in units of radian); $\mu_\ell = 0$ in this energy region. The used styles of the plotted lines mark results obtained in different approximation utilized in the present work, as follows: dash-dot-dot, HF; dash-dot, SCAT(A@); dash, SCAT(UP); solid, SCAT(CP) (the most complete approximation).

The reader can spot a number of other impressive differences between σ_ℓs, or between σ_{tot}s for $e^- + \mathrm{Ba@C_{60}}$ scattering calculated in each of the utilized approximations, and/or between calculated data for $e^- + \mathrm{Ba@C_{60}}$ scattering, on the one hand, and $e^- + \mathrm{Ne@C_{60}}$ and $e^- + \mathrm{Xe@C_{60}}$ scattering, on the other hand.

In summary, similar to the earlier commentary on the differences between electron scattering off Ne@C_{60} and Xe@C_{60}, the highlighted features of electron scattering off Ba@C_{60} underpin, on a bigger scale, the effect of a greater size and polarizability of a compact encapsulated atom A on $e^- + A\mathrm{@C_{60}}$ scattering.

IV. CONCLUSION

The present work provides researchers with the physically transparent, relatively simple, and reasonably complete

approximation applicable to the problem of low-energy electron elastic scattering off endohedral fullerenes $A@C_N$. One of the important elements, inherent to the developed approximations, is the ability to account for coupling between the electrons of C_N and atom A without reference to complicated details of the electronic structure of C_N itself. As of today, the present study provides the most complete information about features of low-energy $e^- + A@C_{60}$ elastic scattering brought about by the confinement-related, static-related, and polarization-related impacts of the individual and coupled members of $A@C_{60}$ on electron elastic scattering off this complex target. Each of them brings specific features into $e^- + A@C_{60}$ scattering. Spectacular effects in the scattering process, primarily associated with polarization of $A@C_{60}$ by an incident electron, have been unraveled, scrutinized, and thoroughly detailed both quantitatively and qualitatively in a physically transparent manner.

We accounted for five scattering partial waves with ℓ ranging from 0 to 4 in the calculations (as was stressed in the paper, this number of electronic waves is adequate for the description of electron scattering in the considered electron-energy region), and demonstrated that almost each partial cross section has a deep Ramsauer-type minimum in the $e^- + A@C_{60}$ scattering cross sections. It is important to emphasize that the revealed effect in $e^- + A@C_{60}$ scattering is much more interesting than the similar effect in low-energy electron scattering off a free atom, because it permits us to separate the contribution of different partial ℓ-electronic waves in the angle-differential scattering cross section, since the position of a minimum depends on the scattering angle.

A practical application of the developed in the present work formalism to the calculation of $e^- + A@C_{60}$ scattering is getting increasingly complicated with increasing number of the partial electronic ℓ waves included into the calculation. Nevertheless, to cover a broader region of electron energies with the aim to get a deeper insight into general features of $e^- + A@C_{60}$ scattering, we accounted for scattering electronic waves up to a g wave in the performed calculations. The contribution of this wave proved to be rich in structure.

One of the results is that not only the individual impacts of polarization of the atom A and C_{60} on $e^- + A@C_{60}$ scattering are generally important, but the correction term to $e^- + A@C_{60}$ scattering, brought about by interference of polarizabilities of the atom A and C_{60}, is essential. The significance of the impact of interference of polarizabilities of C_{60} and A on electron scattering increases essentially with increasing polarizability of the atom A. The interference of polarizability leads to a strong violation of the phase additivity rule.

The results of this paper demonstrate that the interference of polarizabilities is an observable strong effect. A good example proved to be $Ba@C_{60}$ where this effect modifies considerably, both quantitatively and qualitatively, the partial cross sections for $e^- + Ba@C_{60}$ scattering at lower energies, but largely annihilates the whole polarization impact on scattering of s-, p-, d-, and f-partial waves at higher energies.

Lastly, in the present work, we performed the numeric calculations of scattering phases $\delta_\ell(\epsilon)$ down to very low incoming energies ϵ of about 0.001 Ry. By considering the trend of scattering phases at these electron energies and extrapolating their values to the zero energy, we now make the prediction of the existence of negative ions $A@C_{60}^-$ of different total angular momenta. To do so, let us refer to the well-known Levinson theorem in scattering theory [17]. In its generalized form, the Levinson theorem can be written as $\delta_\ell(\epsilon)|_{\epsilon\to 0} \to (N_{n_\ell} + q_\ell)\pi$. Here, N_{n_ℓ} is the number of closed subshells with given ℓ in the ground-state configuration of the encapsulated atom, whereas q_ℓ is the number of additional *empty* bound states with the same ℓ in the field of $A@C_{60}$. By comparing the final values of calculated phases (solid lines in Figs. 4–6) at $\epsilon \to 0$ with the characteristic values of $N_{n\ell}\pi$ for Ne, Xe, and Ba, one can easily conclude about the existence of fullerenes anions $Ne@C_{60}^-$, $Xe@C_{60}^-$, and $Ba@C_{60}^-$ where the attached electron resides either in the state s, or p, or d, or f.

The authors hope that the present work will prompt other theorists to perform more rigorous calculations of $e^- + A@C_{60}$ scattering. We urgently need experimental data on this process. We do hope that the result of this paper will stimulate experimentalists to perform corresponding measurements.

ACKNOWLEDGMENT

V.K.D. acknowledges the support by NSF Grant No. PHY-1305085.

[1] V. K. Dolmatov, M. B. Cooper, and M. E. Hunter, Electron elastic scattering off endohedral fullerenes $A@C_{60}$: The initial insight, J. Phys. B **47**, 115002 (2014).

[2] V. K. Dolmatov, C. Bayens, M. B. Cooper, and M. E. Hunter, Electron elastic scattering and low-frequency bremsstrahlung on $A@C_{60}$: A model static-exchange approximation, Phys. Rev. A **91**, 062703 (2015).

[3] M. Y. Amusia and L. V. Chernysheva, On the behavior of scattering phases in collisions of electrons with multiatomic objects, JETP Lett. **101**, 503 (2015).

[4] V. K. Dolmatov, M. Y. Amusia, and L. V. Chernysheva, Electron elastic scattering off $A@C_{60}$: The role of atomic polarization under confinement, Phys. Rev. A **92**, 042709 (2015).

[5] M. Y. Amusia and L. V. Chernysheva, Role of a fullerene shell upon stuffed atom polarization potential, JETP Lett. **103**, 260 (2016).

[6] A. A. Abrikosov, L. P. Gorkov, and I. E. Dzyaloshinski, in *Methods of Quantum Field Theory in Statistical Physics*, edited by R. A. Silverman (Prentice-Hall, Englewood Cliffs, NJ, 1963).

[7] M. Y. Amusia and L. V. Chernysheva, *Computation of Atomic Processes: A Handbook for the ATOM Programs* (IOP, Bristol, UK, 1997).

[8] J.-P. Connerade, V. K. Dolmatov, and S. T. Manson, A unique situation for an endohedral metallofullerene, J. Phys. B **32**, L395 (1999).

[9] B. Li, G. O'Sullivan, and C. Dong, Relativistic R-matrix calculation photoionization cross section of Xe and Xe@C_{60}, J. Phys. B **46**, 155203 (2013).

[10] V. K. Dolmatov and D. A. Keating, Xe 4*d* photoionization in Xe@C_{60}, Xe@C_{240}, and Xe@C_{60}@C_{240}, J. Phys.: Conf. Ser. **388**, 022097 (2012).

[11] T. W. Gorczyca, M. F. Hasoglu, and S. T. Manson, Photoionization of endohedral atoms using R-matrix methods: Application to Xe@C_{60}, Phys. Rev. A **86**, 033204 (2012).

[12] C. Winstead and V. McKoy, Elastic electron scattering by fullerene, C_{60}, Phys. Rev. A **73**, 012711 (2006).

[13] V. K. Dolmatov, M. B. Cooper, and M. E. Hunter, $e + C_{60}$ and $e + A@C_{60}$ elastic scattering versus the parameters of the C_{60}-model-square-well potential, J. Phys.: Conf. Ser. **635**, 112008 (2015).

[14] G. F. Drukarev, *Collisions of Electrons with Atoms and Molecules, Physics of Atoms and Molecules* (Springer, New York, 1987), p. 252.

[15] M. Y. Amusia and A. S. Baltenkov, On the possibility of considering the fullerene shell C_{60} as a conducting sphere, Phys. Lett. A **360**, 294 (2006).

[16] J. Mitroy, M. S. Safronova, and C. W. Clark, Theory and applications of atomic and ionic polarizabilities, J. Phys. B **43**, 202001 (2010).

[17] L. D. Landau and E. M. Lifshitz, *Quantum Mechanics: Nonrelativistic Theory* (Butterworth-Heinemann, Boston, 2002).